



Ferroptosis is involved in passive Heymann nephritis in rats

Xiujie Shi^{a,1}, Qi Zhang^{a,1}, Meiyang Chang^a, Yifan Zhang^{a,b}, MingMing Zhao^a, Bin Yang^{c,*}, Peng Li^d, Yu Zhang^{a,e,**}

^a Department of Nephrology, Xiyuan Hospital, China Academy of Chinese Medical Sciences, Beijing, 100091, China

^b Beijing University of Chinese Medicine, Beijing, 100029, China

^c Department of Pathology, Xiyuan Hospital, China Academy of Chinese Medical Sciences, Beijing, 100091, China

^d Experimental Research Center, Xiyuan Hospital, China Academy of Chinese Medical Sciences, Beijing, 100091, China

^e Xin-Huangpu Joint Innovation Institute of Chinese Medicine, Guangzhou, 510535, China

ARTICLE INFO

Keywords:

Ferroptosis
Ferritinophagy
Passive Heymann nephritis
Membranous nephropathy

ABSTRACT

Ferroptosis is found to be involved in some experimental models of kidney diseases, but its role in membrane nephropathy (MN) is still unclear. The purpose of this study is to explore whether ferroptosis occurred in MN, and the role of ferritinophagy. In this study, passive Heymann nephritis (PHN) rats were induced by single tail vein injection of anti-Fx1A serum, and normal rats were used as control. The changes of 24 h urinary protein, serum biochemical parameters, renal pathological damage, iron content, lipid peroxidation parameters, ferroptosis markers, and ferritinophagy markers were evaluated in the two groups. Compared with the control group, PHN rats showed obvious proteinuria, hypoproteinemia, and hyperlipidemia. Besides, more severe renal pathological damage and higher Fe²⁺ levels were observed in PHN rats, and the levels of malondialdehyde (MDA) increased significantly, while the levels of superoxide Dismutase (SOD) and glutathione (GSH) decreased. In addition, the expression of glutathione peroxidase 4 (GPX4) in renal tissues of PHN rats decreased significantly, while the expression of transferrin receptor (TFR) and acyl-CoA synthetase long-chain family member 4 (ACSL4) increased. The expression of microtubule associated protein 1 light chain 3 (LC3) II/LC3I and nuclear receptor coactivator 4 (NCOA4) increased significantly. Therefore, our study shows that ferroptosis is involved in the pathological damage of MN, and accompanied by activation of ferritinophagy.

1. Introduction

Membrane nephropathy (MN) is an autoimmune disease that affects the glomerulus and is the main cause of adult nephrotic syndrome. It is mainly manifested by the deposition of immune complexes in the upper and subcutaneous areas, accompanied by local complement activation, podocyte injury, and diffuse thickening of the glomerular basement membrane (GBM) [1]. In the past decade, the incidence of MN in China has continued to rise, and has turned into the fastest growing disease among primary glomerular diseases [2]. In recent years, a large number of clinical and animal experiments explored the etiology and pathogenesis of MN, such as the identification of multiple renal endogenous autoantibodies, providing a more specific strategy for the precise treatment of MN [3].

* Corresponding author. Department of Pathology, Xiyuan Hospital, China Academy of Chinese Medical Sciences, Beijing, 100091, China.

** Corresponding author. Department of Nephrology, Xiyuan Hospital, China Academy of Chinese Medical Sciences, Beijing, 100091, China.

E-mail addresses: yangbin555@126.com (B. Yang), zhangyu8225@126.com (Y. Zhang).

¹ These authors contributed equally to this work.

<https://doi.org/10.1016/j.heliyon.2023.e21050>

Received 22 April 2023; Received in revised form 4 October 2023; Accepted 13 October 2023

Available online 17 October 2023

2405-8440/© 2023 The Author(s). Published by Elsevier Ltd. This is an open access article under the CC BY-NC-ND license (<http://creativecommons.org/licenses/by-nc-nd/4.0/>).

However, there are still many unsolved problems in the potential molecular mechanisms, including autoimmune response, podocyte injury, and immune complex deposition in GBM.

Ferroptosis is a new type of cell death, which is characterized by iron accumulation and lipid peroxidation. Cytomorphology mainly shows mitochondrial membrane rupture, reduced volume, increased membrane density, etc. [4]. The process of ferroptosis is that the inactivation of glutathione peroxidase 4 (GPX4) leads to the disorder of lipid oxide metabolism in cells, and then the generated hydrogen peroxide and Fe^{2+} are catalyzed by Fenton reaction, leading to a large amount of iron deposition, producing a large amount of lipid reactive oxygen species (ROS), destroying the redox balance, and triggering cell death [5,6]. In recent years, the role of ferroptosis in renal diseases has gradually attracted attention. Wang et al. established a rat model with 5/6 nephrectomy and found that the kidney tissue of rats had obvious ferroptosis characteristics, including iron deposition, mitochondrial defects, lipid peroxidation, etc, and inhibition of ferroptosis could significantly improve the renal function and alleviate renal fibrosis of rats, and the effect was independent of apoptosis [7]. Zhang et al. found that oxidative stress injury and iron deposition were involved in podocytes induced by high glucose, and inhibition of ferroptosis reduced podocyte dysfunction [8]. It can be seen that ferroptosis existed in some experimental models of kidney diseases. However, the role of ferroptosis in membranous nephropathy has not been studied.

The deposition of iron ions is one of the main characteristics of ferroptosis, and the metabolism of iron ions plays an important role in regulating ferroptosis. When a large amount of free Fe^{2+} accumulates in cells, it is easy to induce Fenton reaction, leading to ferroptosis. Autophagy, as a cell decomposition process that maintains normal physiological activities and homeostasis in cells, can degrade ferritin, release iron ions, and induce ferroptosis, which is called ferritinophagy [9]. Nuclear receptor coactivator 4 (NCOA4) is a cargo receptor of ferritinophagy, which can detain iron containing ferritin complex into autophagosome, degrade ferritin, release a large number of divalent iron ions, and induce ferroptosis [10]. In a rat model of renal ischemia-reperfusion injury, NACO4 mediated ferritinophagy promoted the occurrence of ferroptosis [11].

Rat passive Heymann nephritis (PHN) is the most commonly used animal model of human membranous nephropathy, induced by injection of anti-Fx1A serum [12,13]. PHN rat model has similar pathogenesis and clinical manifestations to human MN. Anti-Fx1A can bind with antigens on podocyte to form immune complexes that deposit in the glomerulus, leading to kidney damage.

Based on the above researches, a rat model of PHN was applied and we detected various biochemical parameters, renal histopathological changes, ferroptosis and ferritinophagy related markers, to evaluate the role of ferroptosis and ferritinophagy in PHN rats, and enrich the potential mechanism of ferroptosis in kidney diseases.

2. Materials and methods

2.1. Reagents and antibodies

Sheep anti-rat Fx1A serum antibody (PTX-002S, Probetex, San Antonio, USA), BCA protein concentration determination kit (WLA019, wanleibio, shenyang, China), SDS-PAGE gel rapid preparation kit (WLA013, wanleibio, shenyang, China), GPX4 antibody (ab125066, abcam, Cambridge, UK), Transferrin receptor (TFR) antibody (T56618, abmart, shanghai, China), Acyl-CoA synthetase long-chain family member 4(ACSL4) antibody (abcam, ab155282, Cambridge, UK), NCOA4 antibody (A5695, ABclonal, Boston, USA), LC3 antibody (WL01506, wanleibio, shenyang, China), p62 antibody (WL02385, wanleibio, shenyang, China), Sheep anti rabbit IgG HRP (WLA023, wanleibio, shenyang, China), β -actin (WL01845, wanleibio, shenyang, China), ECL luminous liquid (WLA003, wanleibio, shenyang, China), PVDF membrane (IPVH00010, Millipore, Boston, USA), PAS staining solution (WL033, Wanleibio, shenyang, China), The Masson's Trichrome Stain Kit (G1340, Solarbio, Beijing, China), Prussian blue staining kit (G1422, Servicebio, wuhan, China), Iron Assay kit (abcam, Ab83366, Cambridge, UK), SOD Assay kit (A001-1, Nanjing Jiancheng Bioengineering Research Institute, Nanjing, China), MDA Assay kit (G4300, Servicebio, Wuhan China), GSH Assay kit (A006-2, Nanjing Jiancheng Bioengineering Research Institute, Nanjing, China), TRIPure (RP1001, BioTeke, Beijing, China), BeyoRT II M-MLV reverse transcriptase (D7160L, Beyotime, Shanghai, China), PCR cycler (Exicycler 96, BIONEER, Korea).

2.2. Experimental design and grouping

This experiment was approved by the Ethics Committee of Xiyuan Hospital, China's Academy of Chinese Medical Sciences, and all animal care and experiments were conducted in accordance with the guidelines for the care and use of experimental animals. Sixteen Sprague-Dawley male rats weighing 180 ± 20 g (6 weeks) were purchased from Beijing Vital River Laboratory Animal Technology Co., Ltd., and kept in special pathogen-free animal room with ad libitum access to food and water.

After one week of adaptive feeding, all rats were randomly divided into control group and PHN group. PHN rat model was induced by single tail vein injection of anti-Fx1A serum antibody (0.45 ml/100 g), while rats in the normal group were given the same dose of normal saline by tail vein injection [14]. At the 2nd and 4th week after injection, all rats were put into metabolic cages, and 24 h urine was collected for examination. At the end of the 4th week, all rats were anesthetized after fasting for 12 h. After blood was taken from the abdominal aorta, the right kidney of each rat was immediately taken out, part of which was fixed in 4 % paraformaldehyde for histopathological study, and part of which was put into glutaraldehyde electron microscope solution for transmission electron microscope observation, the rest part was put into liquid nitrogen for subsequent Western blot analysis.

2.3. Biochemical parameter measurement

After taking blood from the abdominal aorta, centrifuged it at 3000 rpm for 15 min, collected serum, and measured the levels of serum albumin (ALB), total protein (TP), serum creatinine (Scr), blood urea nitrogen (BUN), total cholesterol (TCH) and Triglyceride (TG) with a Roche Cobas-800matic biochemical analyzer (Roche Diagnostics GmbH, Mannheim, Germany).

2.4. Histopathological staining

Renal cortex was fixed in 10 % formalin buffer for 48 h, dehydrated, paraffin embedded, and sectioned into 5- μ m slices. Slices were stained with hematoxylin differentiation solution for 3 min, rinsed with tap water for 20 min, stained with eosin reagent for 3 min, and then dehydrated with graded ethanol, transparent with xylene, and sealed with neutral resin. During the PAS staining process, the slices were stained with Schiff's staining solution for 15 min, stained with hematoxylin for 2 min; during the Masson staining process, the slices were stained with Regaud hematoxylin solution for 6 min, acid fuchsin solution for 1 min, and aniline blue staining for 5 min. Then, slices were dehydrated with graded ethanol, transparent with xylene, and sealed with neutral resin. The pathological changes of the glomerulus were observed under a light microscope (DP73, OLYMPUS, Japan). 6 different glomerular fields for each specimen ($\times 200$) were used to perform Masson staining analysis and calculate the relative area of glomerular collagen fibers, collagen volume fraction (CVF) was used to evaluate the quantitative analysis of Masson staining. The Masson-positive area (%) = collagen area/full field area $\times 100$ %. 6 different glomerular fields for each specimen ($\times 200$) were used to perform PAS staining analysis and calculate the area of PAS-positive area. The PAS-positive area (%) = PAS-positive area/glomerular area $\times 100$ %. Image J 2 software was used to quantify the mean percentage positive area between the two groups.

2.5. Transmission electron microscope

Renal cortex was fixed in 2.5 % glutaraldehyde and stored at 4 °C for 24 h. Washed with precooled PBS three times, 15 min each time, and fixed in 1 % osmic acid for 1 h. Wash it with pre cooled PBS, dehydrate it in graded ethanol, embedded and sliced, stained with uranyl acetate for 15 min and lead citrate for 10 min. Washed with double distilled water three times. After drying the ultrathin section, it can be observed under transmission electron microscopy to evaluate the pathological changes of glomerular and mitochondrial ultrastructure.

2.6. Prussian blue staining

The renal cortex was fixed in 10 % formalin buffer for 48 h, dehydrated, paraffin embedded, and sectioned into 5- μ m slices. Giving conventional dehydration and transparency, dyed with Prussian blue working solution for 1 h, washed with distilled water for 3 times. Add Prussian blue dye C drop and dye for 3min. Rinsed with tap water. Dehydrated with absolute ethanol, transparent with xylene, sealed with neutral resin, and observed iron deposition in renal tissue under the light microscope. Integrated optical density (IOD) of ferrous iron deposit areas was measured using Image J 2 software and average densities calculated as IOD/area $\times 100$ % [7]. 6 non repeating fields were analyzed.

2.7. Iron detection

Fresh kidney tissues were immediately homogenized with phosphate buffered saline (PBS). Iron detection buffer was used to homogenize the tissue samples and collected the supernatant after centrifugation. Iron detection kit was used to detect the iron content according to the instructions.

2.8. Assessment of lipid peroxidation indexes

SOD was measured by xanthine oxidase method, MDA was measured by thiobarbituric acid method, and GSH was measured by microenzyme labeling method in the renal tissue sample homogenates using commercial kits.

2.9. Western blot

The total protein was extracted from kidney tissues and quantified with BCA protein detection kit. The same amount of protein samples were loaded into 8 %, 10 %, 15 % SDS-PAGE electrophoresis gels and transferred to PVDF membranes. At room temperature, the membranes were sealed in 5 % skimmed milk for 1 h. Incubated the membranes with the following main primary antibodies at 4 °C overnight: GPX4 (1:5000), TFR (1:2000), ACSL4 (1:10000), NCOA4 (1:1000), LC3 (1:500), p62 (1:400). After washed, incubated the membranes with the corresponding secondary antibodies at room temperature for 45 min, and observed the protein band with ECL kit. The film was scanned, and the optical density of the target band was analyzed with the gel image processing system (Gel Pro Analyzer software).

2.10. Real-time qPCR (RT-qPCR)

Total RNA was isolated from frozen renal tissues using TRIpure reagent, reverse transcribed, and amplified by qPCR. Relative mRNA expression was calculated using the $2^{-\Delta\Delta Ct}$ method. The primers used for qPCR are shown in Table 1.

2.11. Statistics and analysis

All data were expressed as mean \pm standard deviation. All data were first tested for normality. Data conforming to normal distribution shall be subject to the independent sample *t*-test, otherwise Mann Whitney *U* test shall be used. SPSS 21.0 software (IBM Inc., Chicago, Illinois, USA) was used for statistical analysis of data. $P < 0.05$ was considered statistically significant.

3. Results

3.1. PHN rats exhibited higher proteinuria and abnormal biochemical parameters

We measured the 24 h urinary protein (24 h UTP) and serum biochemical parameters in the two groups of rats. The results showed that the 24 h UTP level of PHN rats increased significantly after the tail vein injection of anti-Fx1 serum antibody, especially after 2 weeks of injection (Fig. 1A). The levels of Scr and BUN in PHN rats were not significantly different from those in the control group (Fig. 1B and C). However, the level of ALB and TP in PHN rats decreased significantly, accompanied by an increase of TCH and TG (Fig. 1D, E, F and G). This is consistent with the clinical manifestations of MN.

3.2. PHN rats exhibited more severe renal pathological changes

We evaluated the renal pathological damage of rats with HE (Fig. 2A), PAS (Fig. 2B), and Masson staining (Fig. 2C). The results showed that the glomerular structure of the control group was complete, and no abnormality was found in the GBM. In PHN rats, the glomerulus volume became significantly larger, the GBM was significantly thickened, some renal tubular epithelial cells were swollen, atrophied, and disappeared. There were protein casts, and a large amount of collagen was deposited in the renal interstitium and glomerulus. The positive area of PAS and Masson staining increased significantly (Fig. 2D and E).

The ultrastructure of glomerulus and mitochondria were observed by transmission electron microscopy. In the control group, the foot processes of podocytes were orderly arranged and uniform in size, the thickness of GBM was uniform, and no electronic densification was deposited (Fig. 3A). The Mitochondria have a double membrane structure with normal volume and transparent cristae, and ribosomes are arranged in order (Fig. 3B). In PHN rats, the GBM was clearly thickened, electronic densification was deposited under the epithelium, and the foot processes of podocytes were fused and detached (Fig. 3C). Autolysosome was observed. The volume of mitochondria decreased, the outer membrane broken, and the mitochondrial cristae decreased or disappeared, which were consistent with the characteristics of ferroptosis (Fig. 3D).

3.3. PHN rats exhibited iron deposition and lipid peroxidation in renal tissue

Next, we used Prussian blue staining and iron detection kit to detect whether there was iron deposition in the kidney tissues of rats in the two groups. The nucleus and other tissues were red after Prussian blue staining, while the deposition site of iron was blue (Fig. 4A). The positive area of Prussian blue staining increased significantly (Fig. 4B). For iron detection, the results showed that the content of Fe^{2+} in the renal tissue of PHN rats was significantly higher than that of the control group (Fig. 4C), indicating that PHN rats had obvious iron deposition. In addition, we detected the levels of SOD (Fig. 4D), GSH (Fig. 4E) and MDA (Fig. 4F) in the kidney tissues of the two groups. The results showed that the level of MDA in the PHN rats increased significantly, while the levels of SOD and GSH decreased, which indicated that lipid peroxidation occurred in the kidney, which were also the characteristics of ferroptosis.

4. Ferroptosis occurred in PHN rats

We explored the expression of GPX4, TFR, and ACSL4, which were the biomarkers of ferroptosis. GPX4 can convert lipid hydroperoxides into non-toxic lipid alcohols with glutathione (GSH), thus protecting cells from ferroptosis. TFR is a key protein receptor

Table 1
Sequence of primer pairs used for gene amplification.

Target gene	Forward primer (5'–3')	Reverse primer (5'–3')
GPX4	AGTTCGGGAGGCAGGAG	CCACGAGCCGTTCTTA
ACSL4	TCCGCTGTGACTTAT	ACTTGGAGGAATGCTTG
TFR	ACTATGGAGCTGTTGGTGC	ATCAATCGGATGCTTTACG
NCOA4	AGACTACGGCTCCTGCTA	CTGACTAAGGTTTCCCACT
p62	ATGCCTTTGGCTTTTTTCGCA	GGGAAAGTCCGGCAAGTGTA
β -actin	GGAGATTACTGCCCTGGCTCCTAGC	GGCCGGACTCATCGTACTCCTGCTT

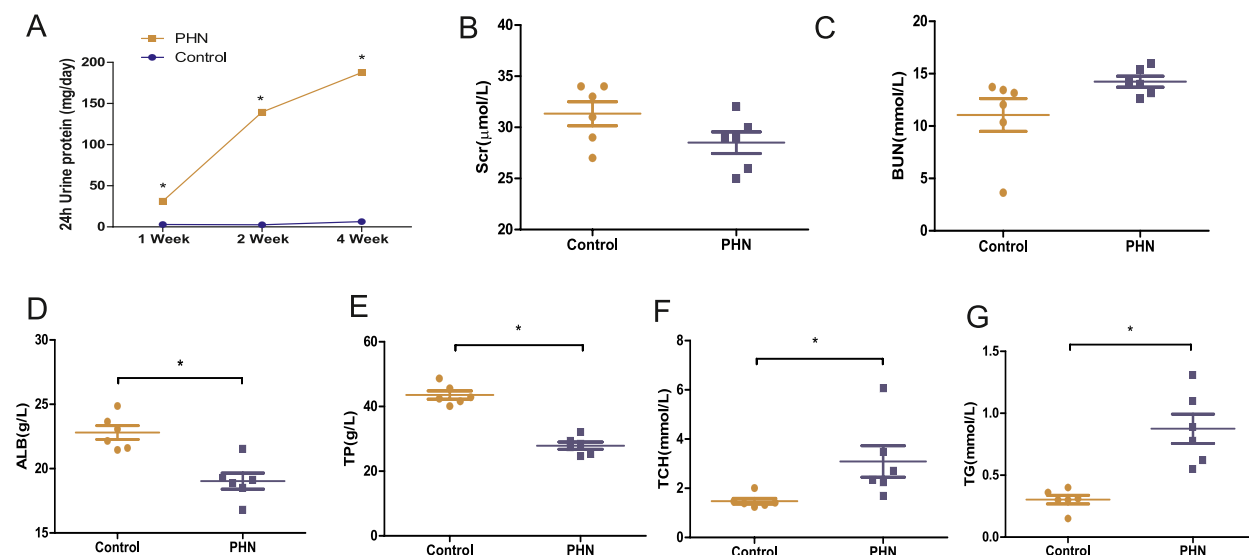


Fig. 1. PHN rats exhibited higher proteinuria and abnormal biochemical parameters. **Note:** (A) 24 h urine protein ($n = 8$); Serum levels of Scr (B, $n = 6$), BUN (C, $n = 6$), ALB (D, $n = 6$), TP (E, $n = 6$), TCH (F, $n = 6$) and TG (G, $n = 6$). * $P < 0.05$ vs. control group. PHN, passive Heymann nephritis; 24 h, UTP, 24 h urinary protein; Scr, serum creatinine; BUN, blood urea nitrogen; ALB, albumin; TP, total protein; TCH, total cholesterol; TG, triglyceride.

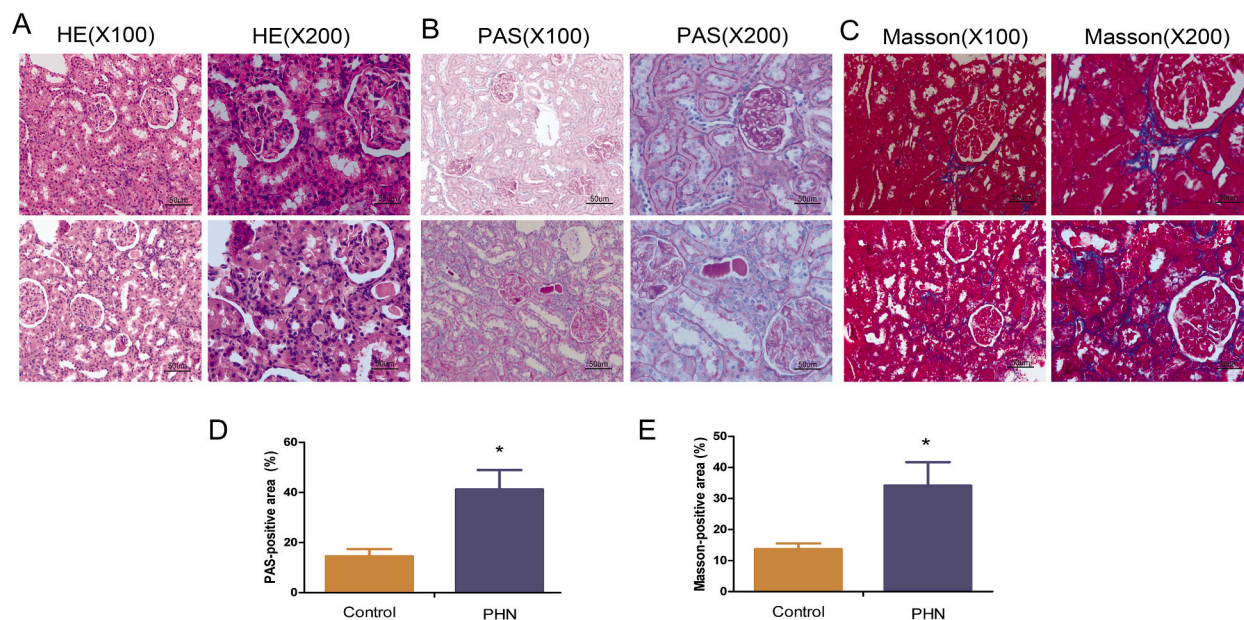


Fig. 2. PHN rats exhibited more severe renal pathological changes. **Note:** (A) HE staining of renal tissue ($\times 100$ and $\times 200$); (B) PAS staining of renal tissue ($\times 100$ and $\times 200$); (C) Masson staining of renal tissue ($\times 100$ and $\times 200$); (D) The ratio of PAS staining positive area ($n = 6$); (E) The ratio of Masson staining positive area ($n = 6$). * $P < 0.05$ vs. control group. PHN, passive Heymann nephritis; HE, hematoxylin eosin; PAS, Periodic Acid Schiff stain.

responsible for extracellular Fe^{3+} input. Its increase indicates that it increased the level of intracellular iron ions, leading to iron deposition. ACSL4 can promote the cascade reaction of PUFAs through arachidonic acid and adrenal acid, generate cytotoxic lipid hydroperoxide, and promote ferroptosis [15]. The Western blot results showed that the protein expression of GPX4 in PHN rat kidney tissues decreased, while the expression of TFR and ACSL4 increased (Fig. 5A and B). Besides, the mRNA showed the same results with Western blot, indicating the occurrence of ferroptosis in PHN rats (Fig. 5C, D and E).

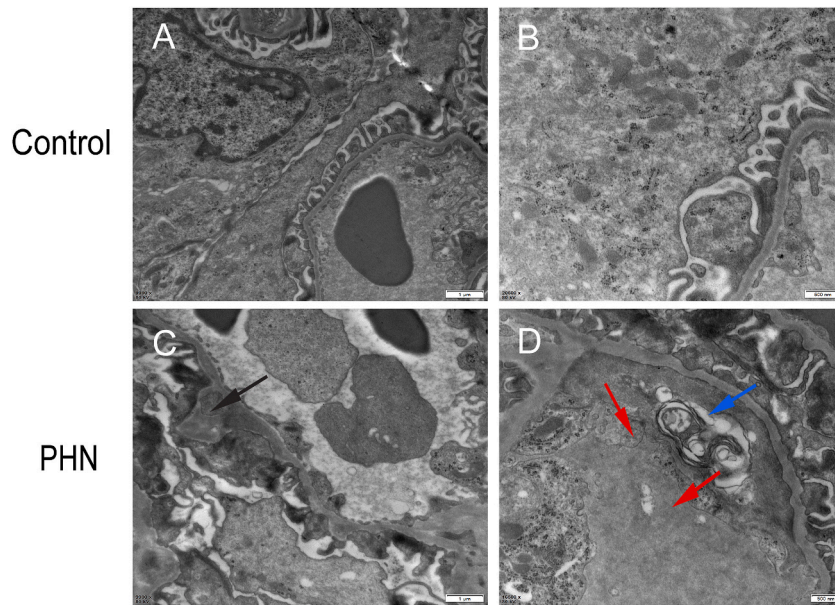


Fig. 3. PHN rats exhibited more severe renal tissue structural damage under transmission electron microscopy. **Note:** A and C: 9900 \times , Scar bar, 1 μ m; B and D, 20500 \times , Scar bar, 500 nm; Black arrow: thickened GBM, deposition of electronic densification, fused and detached foot processes of podocytes. Blue arrow: autolysosome; Red arrow: decreased mitochondria volume, broken outer membrane, decreased or disappeared mitochondrial cristae. PHN, passive Heymann nephritis.

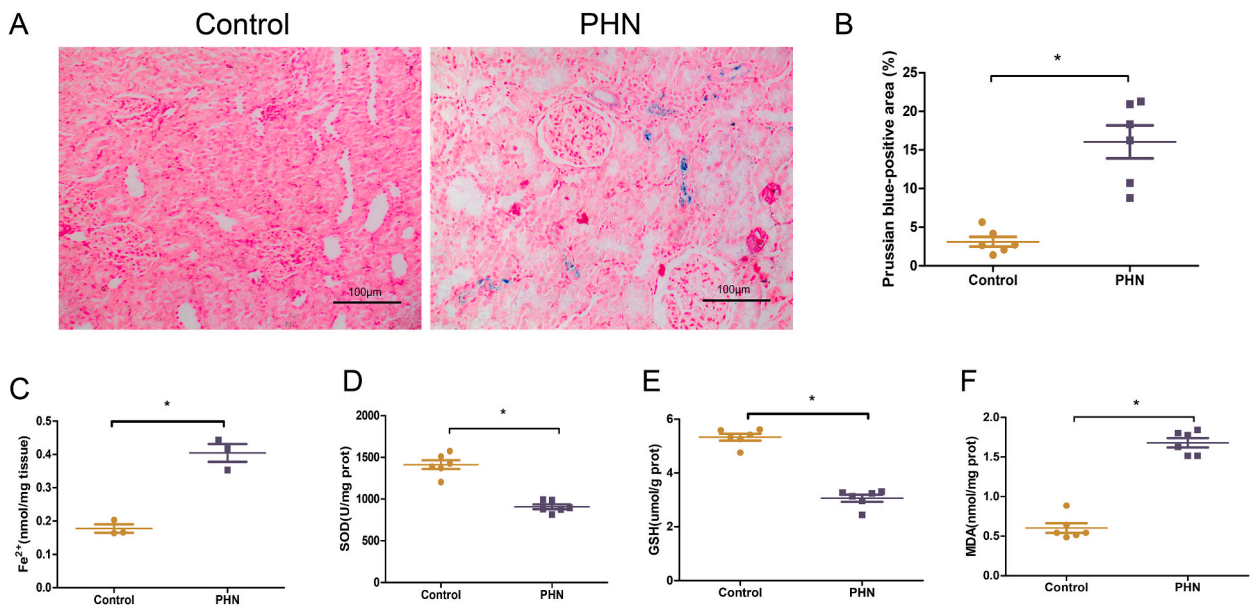


Fig. 4. PHN rats exhibited significant iron deposition and lipid peroxidation in renal tissue. **Note:** (A) Prussian blue staining; (B) The ratio of Prussian blue-positive area ($n = 6$). (C) Fe^{2+} in renal tissues ($n = 3$). The SOD (D, $n = 6$), GSH (E, $n = 6$), and MDA (F, $n = 6$) concentrations in the kidney tissue lysates. * $P < 0.05$ vs. control group. PHN, passive Heymann nephritis; SOD, Superoxide Dismutase; MDA, malondialdehyde.

4.1. Ferritinophagy was activated in PHN rats

We preliminarily explored whether ferroptosis in PHN rats was related to ferritinophagy. LC3 and p62 are common markers for evaluating autophagic activity. The conversion of cytosol LC3-I to membrane binding LC3-II indicates the formation of autophage. p62 is an autophagic substrate that can interact with LC3 to enter autophage and degrade through autolysosome [16]. NCOA4 is a cargo receptor that mediates ferritinophagy, Increased expression of NCOA4 will promote the degradation of ferritin, leading to iron

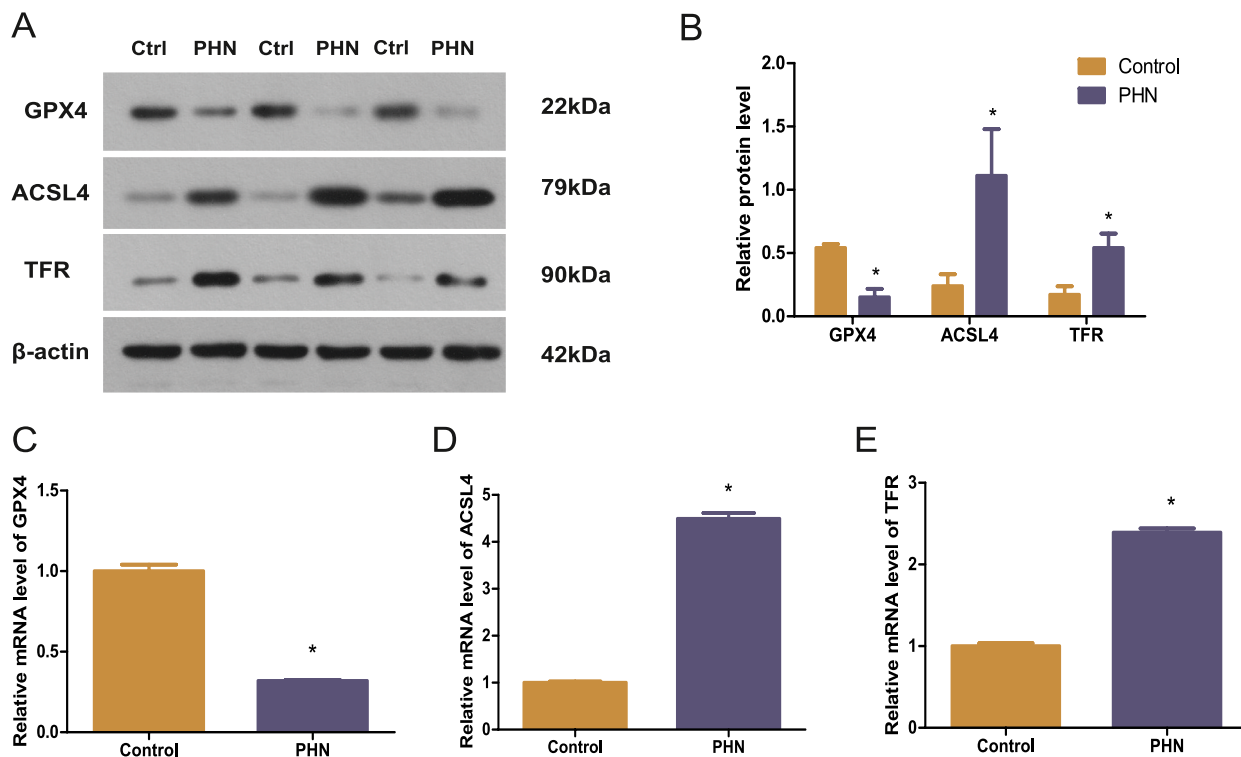


Fig. 5. Ferroptosis occurred in PHN rats. **Note:** Western blotting bands (A) and analysis(B) of GPX4, ACSL4, and TFR ($n = 3$). The original uncropped blot images are shown in Fig. S1. mRNA expression of GPX4 (C, $n = 3$), ACSL4(D, $n = 3$) and TFR (E, $n = 3$) ($n = 3$). * $P < 0.05$ vs. control group. Ctrl, control; PHN, passive Heymann nephritis; GPX4, glutathione peroxidase 4; ACSL4, acyl-CoA synthetase long-chain family member 4; TFR, transferrin receptor.

deposition, and inducing ferroptosis [17]. The results of this study showed that the ratio of LC3II/LC3I and the expression of NCOA4 in PHN rats kidney tissues increased significantly, and the expression of p62 increased, but there was no statistical significance compared with the normal group (Fig. 6A and B). Besides, the mRNA expressions of p62 and NCOA4 both increased significantly (Fig. 6C and D). The above results indicate that autophagy of ferritin was activated in PHN rats.

5. Discussion

In most patients, MN is an autoimmune disease in which an autocirculating antibody combines with endogenous podocyte antigens to form a sedimentary immune complex [18]. The main clinical features of MN are proteinuria, hypoproteinemia, hyperlipidemia, hematuria, hypertension, etc. Under light microscope, the histomorphology of MN mainly showed diffuse thickening of GBM, and the immunoglobulin and complement components with granular positive. The electronic densification deposits on the outside of the GBM and the extensive fusion and disappearance of foot processes in podocytes can be observed under the transmission electron microscope [19].

PHN rat model is commonly used to simulate the pathogenesis of MN, which activates the complement cascade reaction through the combination of autoantibodies and their target antigens, forming a membrane attacking complex C5b-9, and leading to glomerular damage [20]. In this study, the PHN rat model was induced by a single injection of anti-Fx1 serum antibody into the tail vein. It can be found that PHN rats had obvious proteinuria, accompanied by a significant decrease in ALB and TP, with an increase in TCH and TG, which are typical clinical manifestations of MN. There was no significant difference in Scr and BUN between the two groups. In addition, through histopathological staining, it could be found in PHN rats that the glomerular volume in the renal cortex significantly increased, the GBM thickened, some renal tubular epithelial cells appeared swelling, atrophy and disappearance, there was obvious protein tube type, and a large amount of collagen deposition in the renal interstitium and glomerulus.

Ferroptosis is a new type of cell death characterized by abnormal accumulation of lipid ROS and deposition of iron. Ferroptosis is mainly manifested by the atrophy of mitochondria, the increase of mitochondrial membrane density, the reduction, degradation or disappearance of Crista, and the rupture of outer membrane in morphological features, which is different from other types of programmed cell death [21]. GPX4 is an important regulator of ferroptosis, which can transform GSH into oxidized glutathione, inhibit the formation of lipid peroxide, and thus protect cells. When the activity of GPX4 decreases, the cytotoxic lipid L-OOH is converted into lipid ROS, and inducing ferroptosis [22]. After ACSL4 is activated, free polyunsaturated fatty acids (PUFAs) can be induced to esterify, and then PUFAs combine with phosphatidylethanolamine (PEs), which is oxide substrate of ferroptosis, enter membrane

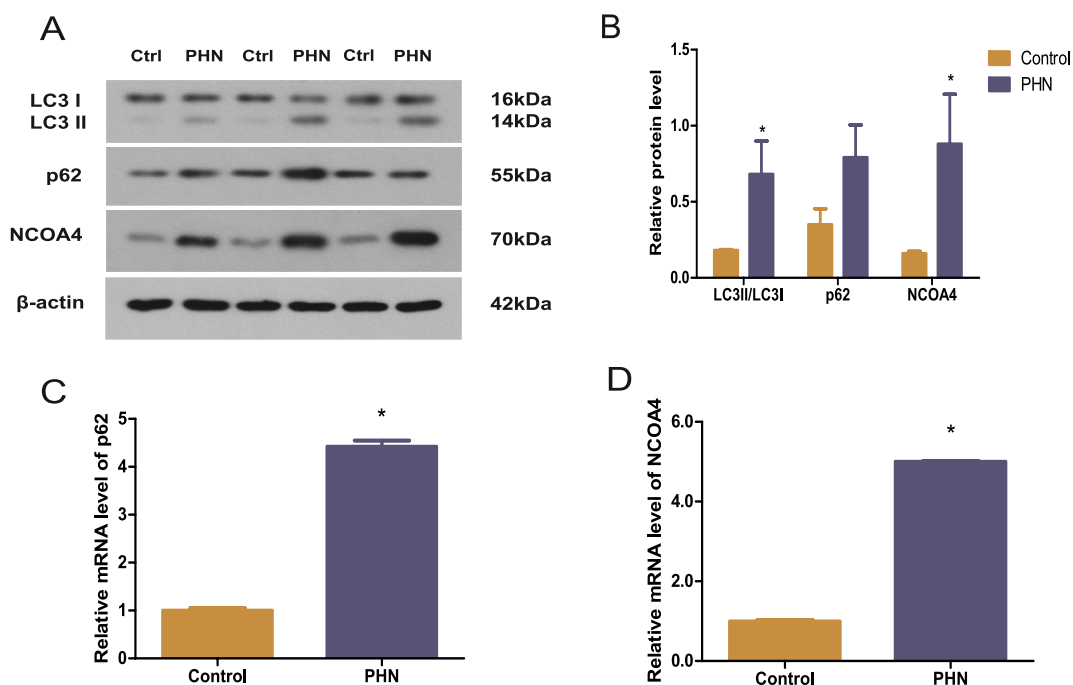


Fig. 6. Ferritinophagy was activated in PHN rats. **Note:** Western blotting bands (A) and analysis (B) of LC3II/LC3I, p62 and NCOA4 ($n = 3$). The original uncropped blot images are shown in Fig. S2. mRNA expression of p62 (C, $n = 3$) and NCOA4 (D, $n = 3$). * $P < 0.05$ vs. control group. Ctrl, control; PHN, passive Heymann nephritis; LC3: microtubule associated protein 1 light chain 3; p62, Sequestosome 1; NCOA4, nuclear receptor coactivator 4.

phospholipids, and induce ferroptosis. Therefore, the upregulation of ACSL4 is considered as a biomarker of ferroptosis [23]. The circulation and utilization of iron ions are closely related to the iron homeostasis in cells. The TFR can take extracellular iron into cells and transport it in the form of ferritin complexes for storage. When TFR increases, it will lead to overload and deposition of iron in cells, leading to ferroptosis [24,25].

Recent studies have emphasized the role of ferroptosis in the pathogenesis of some kidney diseases and experimental models, such as diabetic nephropathy (DN), and IgA nephropathy. Wu et al. found that the levels of serum ferritin, lactate dehydrogenase (LDH), ROS, and MDA in DN patients significantly increased, accompanied by increased mRNA levels of ACSL4 and decreased mRNA levels of GPX4 [26]. Wu et al. found that the fluorescence expression of GPX4 was significantly reduced in renal tissues of patients with IgA nephropathy. In mesangial cells stimulated by galactose deficient IgA1(Gd IgA1), the expression of GPX4 and GSH decreased, while ACSL4, ROS and MDA significantly increased [27]. Kidneys of lupus nephritis patients and immune complex glomerulonephritis mice showed increased lipid peroxidation, increase in ACSL4, and decrease in GPX4 [28]. In addition, ferroptosis suppresses the immune system by reducing the number of T and B cells, and has important potential in the treatment of immune system diseases [29]. Ferroptosis has also been found in podocytes, whose damage induced by immune complexes is a core process in the pathogenesis of MN. However, there is no such study to explore the role of ferroptosis in MN.

In this study, we found that the mitochondria of PHN rats showed decreased volume, rupture of the outer membrane, and reduction or disappearance of mitochondrial cristae, which were the characteristics of ferroptosis. In addition, there was Fe^{2+} deposition in kidney tissues of PHN rats, which could be seen by Prussian blue staining and iron detection. In addition, the level of MDA in the PHN rats increased, while the levels of SOD and GSH decreased, which indicated that lipid peroxidation occurred in the kidney, which provided extra evidences of ferroptosis. Besides, Western blotting results showed that compared with the control group, the protein expression of GPX4 in renal tissues of PHN rats decreased significantly, while the ACSL4 and TFR increased significantly, and the mRNA expression of GPX4, ACSL4 and TFR showed the same results. These results indicated that ferroptosis occurred in PHN rats.

Recent studies show that ferritinophagy plays a role in ferroptosis by regulating iron ion metabolism. NCOA4 is a selective cargo receptor for ferritinophagy, which can be activated by autophagy related genes to guide ferritin into autophagy and then release Fe^{2+} by degrading ferritin [30]. In LPS induced renal tubular epithelial cells, accumulation of Fe^{2+} and lipid peroxidation were observed, accompanied by increased expression of NCOA4 [31].

LC3 and p62 are widely used to evaluate autophagic activity. Transformation of LC3-I into membrane LC3-II indicates the formation of autophagy, therefore the ratio of LC3-II/I was positively correlated with autophagy level. As an autophagic substrate, p62 is selectively encapsulated in autophages, and then degraded by proteolytic enzymes in autolysosome [32]. Therefore, when autophagic activity increases, p62 generally decreases. Previous studies have observed reduced autophagy activity in MN [33], but autophagy has a double-sided effect, and excessive autophagy can also promote cell death [34]. Therefore, we explored the role of ferritin autophagy in MN.

In this study, we evaluated the expression of ferritinophagy markers in PHN rats. The results showed that the protein levels of NCOA4 and LC3-II/I in the PHN rats significantly increased, while the expression of p62 increased with no statistical significance. But the mRNA expressions of p62 and NCOA4 both increased significantly. The increase of LC3-II/I indicated the formation of autophagy, and the upstream of autophagy is active. The enhancement of p62 generally indicates the dysfunction of autophagy and lysosomes, and the inhibition of autophagy activity. However, as a stress protein, under the conditions of toxic substances and oxidative stress, increased p62 expression and activated autophagy can also occur simultaneously [35,36]. Ishii T et al. showed that under oxidative stress conditions, nuclear factor erythroid 2-related factor 2 (Nrf2) was activated to cope with oxidative stress damage. Nrf2 could induce an increase in the expression of p62, and knock of Nrf2 inhibited the expression of p62 in cells [37]. In turn, p62 could bind to Keap1 through KIR region, activate Nrf2, and further increased the expression of itself [38]. Considering that lipid peroxidation is one of the main characteristics of ferroptosis, the increased expression of p62 may be related to oxidative stress, which, of course, needs further exploration. In conclusion, the above results indicated that ferritinophagy was activated in PHN rats (Fig. 7).

However, this study still has the following shortcomings: 1) No ferroptosis inducer or inhibitor was used to further explore the role of ferroptosis in PHN rats; 2) The mechanism of autophagy is relatively complex, and further exploration is needed to prove the enhancement of ferritinophagy, by detecting the autophagy related genes (such as ATG3, ATG5) that involved in NCOA4 mediated autophagy, and the level of ferritin; 3) No inducers or inhibitors of ferritinophagy were applied; 4) No further validation in cells.

6. Conclusion

Our study suggests that ferroptosis is involved PHN rats, and accompanied by activation of ferritinophagy. This provides novel insights for understanding the pathogenesis of MN, and also broadens the field of ferroptosis in kidney diseases.

Ethical statement

This experiment was approved by the Ethics Committee of Xiyuan Hospital, China's Academy of Chinese Medical Sciences (CACMA) (2022XLC031-1).

Funding statement

This work was supported by CACMS Innovation Fund (Grant Number: CI2021A01206), the Joint Innovation Fundation of Joint Innovation Institute of Chinese (JIICM) (Grant Number:2021IR009) and Beijing Natural Science Foundation (Grant Number: 7232315).

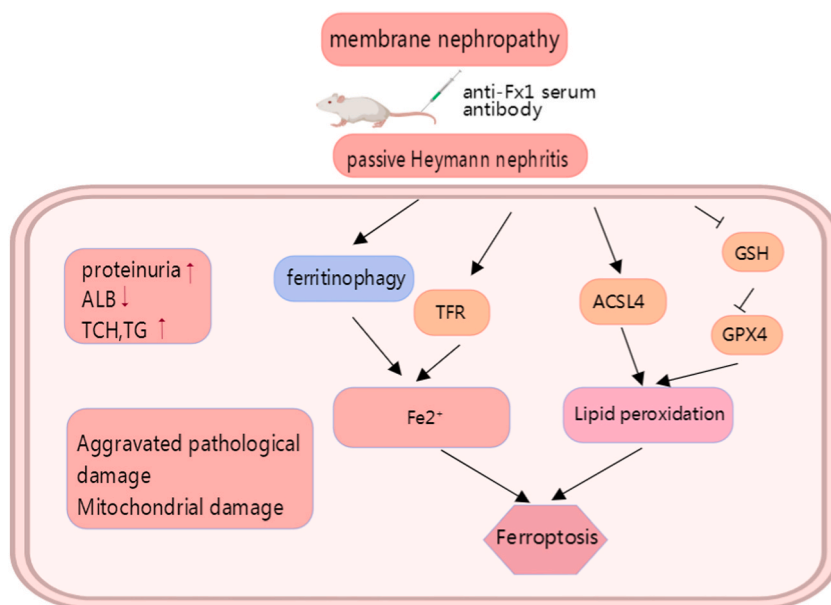


Fig. 7. Ferroptosis is Involved in Passive Heymann Nephritis in Rats. **Note:** A rat model of PHN induced by injection of anti-Fx1A antibody. PHN rats exhibit increased proteinuria, TCH and TG, decreased albumin, aggravated pathological damage and mitochondria mitochondrial damage. In PHN rats, TFR increases level of Fe^{2+} , then excessive Fe^{2+} , activated ACSL4, reduced synthesis of GSH and decreased GPX4 activity induce ferroptosis. Activation of ferritinophagy releases a large number of Fe^{2+} and induces ferroptosis. PHN, passive Heymann nephritis; ALB, albumin; TCH, total cholesterol; TG, triglyceride; TRF, transferrin; ACSL4, acyl-CoA synthetase long-chain family member 4; GSH, glutathione; GPX4, glutathione peroxidase 4.

Data availability statement

All data generated or analyzed during this study are available from the corresponding author on reasonable request.

CRedit authorship contribution statement

Xiujie Shi: Conceptualization, Formal analysis, Methodology, Writing – original draft. **Qi Zhang:** Data curation, Formal analysis, Methodology. **Meiying Chang:** Methodology, Project administration, Resources. **Yifan Zhang:** Formal analysis, Methodology, Project administration. **MingMing Zhao:** Formal analysis, Methodology, Supervision. **Bin Yang:** Data curation, Formal analysis, Supervision, Writing – review & editing. **Peng Li:** Formal analysis, Methodology, Supervision. **Yu Zhang:** Conceptualization, Data curation, Supervision, Writing – review & editing, Resources.

Declaration of competing interest

The authors declare that they have no known competing financial interests or personal relationships that could have appeared to influence the work reported in this paper.

Appendix A. Supplementary data

Supplementary data to this article can be found online at <https://doi.org/10.1016/j.heliyon.2023.e21050>.

References

- [1] P. Ronco, L. Beck, H. Debiec, F.C. Fervenza, F.F. Hou, V. Jha, S. Sethi, A. Tong, M. Vivarelli, J. Wetzels, Membranous nephropathy, *Nat. Rev. Dis. Prim.* 7 (2021) 69, <https://doi.org/10.1038/s41572-021-00303-z>.
- [2] X. Xu, G. Wang, N. Chen, T. Lu, S. Nie, G. Xu, P. Zhang, Y. Luo, Y. Wang, X. Wang, J. Schwartz, J. Geng, F.F. Hou, Long-term exposure to air pollution and increased risk of membranous nephropathy in China, *J. Am. Soc. Nephrol.* 27 (2016) 3739–3746, <https://doi.org/10.1681/ASN.2016010093>.
- [3] P. Zhang, W. Huang, Q. Zheng, J. Tang, Z. Dong, Y. Jiang, Y. Liu, W. Liu, A novel insight into the role of pla2r and thsd7a in membranous nephropathy, *J. Immunol Res* 2021 (2021), 8163298, <https://doi.org/10.1155/2021/8163298>.
- [4] J. Li, F. Cao, H.L. Yin, Z.J. Huang, Z.T. Lin, N. Mao, B. Sun, G. Wang, Ferroptosis: past, present and future, *Cell Death Dis.* 11 (2020) 88, <https://doi.org/10.1038/s41419-020-2298-2>.
- [5] S.J. Dixon, K.M. Lemberg, M.R. Lamprecht, R. Skouta, E.M. Zaitsev, C.E. Gleason, D.N. Patel, A.J. Bauer, A.M. Cantley, W.S. Yang, B.R. Morrison, B.R. Stockwell, Ferroptosis: an iron-dependent form of nonapoptotic cell death, *Cell* 149 (2012) 1060–1072, <https://doi.org/10.1016/j.cell.2012.03.042>.
- [6] W.S. Yang, R. Sriramaratnam, M.E. Welsch, K. Shimada, R. Skouta, V.S. Viswanathan, J.H. Cheah, P.A. Clemons, A.F. Shamji, C.B. Clish, L.M. Brown, A. W. Girotti, V.W. Cornish, S.L. Schreiber, B.R. Stockwell, Regulation of ferroptotic cancer cell death by gpx4, *Cell* 156 (2014) 317–331, <https://doi.org/10.1016/j.cell.2013.12.010>.
- [7] J. Wang, Y. Wang, Y. Liu, X. Cai, X. Huang, W. Fu, L. Wang, L. Qiu, J. Li, L. Sun, Ferroptosis, a new target for treatment of renal injury and fibrosis in a 5/6 nephrectomy-induced ckd rat model, *Cell Death Dis.* 8 (2022) 127, <https://doi.org/10.1038/s41420-022-00931-8>.
- [8] Q. Zhang, Y. Hu, J.E. Hu, Y. Ding, Y. Shen, H. Xu, H. Chen, N. Wu, Sp1-mediated upregulation of prdx6 expression prevents podocyte injury in diabetic nephropathy via mitigation of oxidative stress and ferroptosis, *Life Sci.* 278 (2021), 119529, <https://doi.org/10.1016/j.lfs.2021.119529>.
- [9] W. Hou, Y. Xie, X. Song, X. Sun, M.T. Lotze, H.R. Zeh, R. Kang, D. Tang, Autophagy promotes ferroptosis by degradation of ferritin, *Autophagy* 12 (2016) 1425–1428, <https://doi.org/10.1080/15548627.2016.1187366>.
- [10] J.D. Mancias, X. Wang, S.P. Gygi, J.W. Harper, A.C. Kimmelman, Quantitative proteomics identifies ncoa4 as the cargo receptor mediating ferritinophagy, *Nature* 509 (2014) 105–109, <https://doi.org/10.1038/nature13148>.
- [11] M. Sui, D. Xu, W. Zhao, H. Lu, R. Chen, Y. Duan, Y. Li, Y. Zhu, L. Zhang, L. Zeng, Cirbp promotes ferroptosis by interacting with elavl1 and activating ferritinophagy during renal ischaemia-reperfusion injury, *J. Cell Mol. Med.* (2021), <https://doi.org/10.1111/jcmm.16567>.
- [12] J.A. Jefferson, J.W. Pippin, S.J. Shankland, Experimental models of membranous nephropathy, *Drug Discov. Today Dis. Model.* 7 (2010) 27–33, <https://doi.org/10.1016/j.ddmod.2010.11.001>.
- [13] T.T. Li, X.H. Zhang, J.F. Jing, X. Li, X.Q. Yang, F.H. Zhu, W. Tang, J.P. Zuo, Artemisinin analogue sm934 ameliorates the proteinuria and renal fibrosis in rat experimental membranous nephropathy, *Acta Pharmacol. Sin.* 36 (2015) 188–199, <https://doi.org/10.1038/aps.2014.134>.
- [14] X.H. Wang, R. Lang, Q. Zeng, Y. Liang, N. Chen, Z.Z. Ma, R.H. Yu, Jianpi qushi heluo formula alleviates renal damages in passive hemann nephritis in rats by upregulating parkin-mediated mitochondrial autophagy, *Sci. Rep.* 11 (2021), 18338, <https://doi.org/10.1038/s41598-021-97137-2>.
- [15] X. Jiang, B.R. Stockwell, M. Conrad, Ferroptosis: mechanisms, biology and role in disease, *Nat. Rev. Mol. Cell Biol.* 22 (2021) 266–282, <https://doi.org/10.1038/s41580-020-00324-8>.
- [16] L. Yu, Y. Chen, S.A. Tooze, Autophagy pathway: cellular and molecular mechanisms, *Autophagy* 14 (2018) 207–215, <https://doi.org/10.1080/15548627.2017.1378838>.
- [17] N. Santana-Codina, A. Gikandi, J.D. Mancias, The role of ncoa4-mediated ferritinophagy in ferroptosis, *Adv. Exp. Med. Biol.* 1301 (2021) 41–57, https://doi.org/10.1007/978-3-030-62026-4_4.
- [18] Q. Cai, A.R. Hendricks, Membranous nephropathy: a ten-year journey of discoveries, *Semin. Diagn. Pathol.* 37 (2020) 116–120, <https://doi.org/10.1053/j.semdp.2020.01.001>.
- [19] Z. Xu, L. Chen, H. Xiang, C. Zhang, J. Xiong, Advances in pathogenesis of idiopathic membranous nephropathy, *Kidney Dis.* 6 (2020) 330–345, <https://doi.org/10.1159/000507704>.
- [20] R.A. Sinico, N. Mezzina, B. Trezzi, G.M. Ghiggeri, A. Radice, Immunology of membranous nephropathy: from animal models to humans, *Clin. Exp. Immunol.* 183 (2016) 157–165, <https://doi.org/10.1111/cei.12729>.
- [21] J. Wang, Y. Liu, Y. Wang, L. Sun, The cross-link between ferroptosis and kidney diseases, *Oxid. Med. Cell. Longev.* 2021 (2021), 6654887, <https://doi.org/10.1155/2021/6654887>.
- [22] A.J. Friedmann, M. Schneider, B. Proneth, Y.Y. Tyurina, V.A. Tyurin, V.J. Hammond, N. Herbach, M. Aichler, A. Walch, E. Eggenhofer, D. Basavarajappa, O. Radmark, S. Kobayashi, T. Seibt, H. Beck, F. Neff, I. Esposito, R. Wanke, H. Forster, O. Yefremova, M. Heinrichmeyer, G.W. Bornkamm, E.K. Geissler, S.

- B. Thomas, B.R. Stockwell, V.B. O'Donnell, V.E. Kagan, J.A. Schick, M. Conrad, Inactivation of the ferroptosis regulator gpx4 triggers acute renal failure in mice, *Nat. Cell Biol.* 16 (2014) 1180–1191, <https://doi.org/10.1038/ncb3064>.
- [23] H. Yuan, X. Li, X. Zhang, R. Kang, D. Tang, Identification of acsl4 as a biomarker and contributor of ferroptosis, *Biochem. Biophys. Res. Commun.* 478 (2016) 1338–1343, <https://doi.org/10.1016/j.bbrc.2016.08.124>.
- [24] S.J. Dixon, B.R. Stockwell, The role of iron and reactive oxygen species in cell death, *Nat. Chem. Biol.* 10 (2014) 9–17, <https://doi.org/10.1038/nchembio.1416>.
- [25] J.Y. Cao, S.J. Dixon, Mechanisms of ferroptosis, *Cell. Mol. Life Sci.* 73 (2016) 2195–2209, <https://doi.org/10.1007/s00018-016-2194-1>.
- [26] Y. Wu, Y. Zhao, H.Z. Yang, Y.J. Wang, Y. Chen, Hmgbl regulates ferroptosis through nrf2 pathway in mesangial cells in response to high glucose, *Biosci. Rep.* 41 (2021), <https://doi.org/10.1042/BSR20202924>.
- [27] J. Wu, X. Shao, J. Shen, Q. Lin, X. Zhu, S. Li, J. Li, W. Zhou, C. Qi, Z. Ni, Downregulation of pparalpha mediates fabp1 expression, contributing to iga nephropathy by stimulating ferroptosis in human mesangial cells, *Int. J. Biol. Sci.* 18 (2022) 5438–5458, <https://doi.org/10.7150/ijbs.74675>.
- [28] A.A. Allij, D. Desai, A. Elshika, M. Conrad, B. Proneth, W. Clapp, C. Atkinson, M. Segal, L.A. Searcy, N.D. Denslow, S. Bolisetty, B. Mehrad, L. Morel, Y. Scindia, Kidney tubular epithelial cell ferroptosis links glomerular injury to tubulointerstitial pathology in lupus nephritis, *Clin. Immunol.* 248 (2023), 109213, <https://doi.org/10.1016/j.clim.2022.109213>.
- [29] S. Xu, J. Min, F. Wang, Ferroptosis: an emerging player in immune cells, *Sci. Bull.* 66 (2021) 2257–2260, <https://doi.org/10.1016/j.scib.2021.02.026>.
- [30] N. Li, W. Wang, H. Zhou, Q. Wu, M. Duan, C. Liu, H. Wu, W. Deng, D. Shen, Q. Tang, Ferritinophagy-mediated ferroptosis is involved in sepsis-induced cardiac injury, *Free Radic. Biol. Med.* 160 (2020) 303–318, <https://doi.org/10.1016/j.freeradbiomed.2020.08.009>.
- [31] Y. Tang, H. Luo, Q. Xiao, L. Li, X. Zhong, J. Zhang, F. Wang, G. Li, L. Wang, Y. Li, Isoliquiritigenin attenuates septic acute kidney injury by regulating ferritinophagy-mediated ferroptosis, *Ren. Fail.* 43 (2021) 1551–1560, <https://doi.org/10.1080/0886022X.2021.2003208>.
- [32] B. Levine, G. Kroemer, Biological functions of autophagy genes: a disease perspective, *Cell* 176 (2019) 11–42, <https://doi.org/10.1016/j.cell.2018.09.048>.
- [33] Q. Di Tu, J. Jin, X. Hu, Y. Ren, L. Zhao, Q. He, Curcumin improves the renal autophagy in rat experimental membranous nephropathy via regulating the pi3k/akt/mTOR and nrf2/ho-1 signaling pathways, *BioMed Res. Int.* 2020 (2020), 7069052, <https://doi.org/10.1155/2020/7069052>.
- [34] M.J. Livingston, H.F. Ding, S. Huang, J.A. Hill, X.M. Yin, Z. Dong, Persistent activation of autophagy in kidney tubular cells promotes renal interstitial fibrosis during unilateral ureteral obstruction, *Autophagy* 12 (2016) 976–998, <https://doi.org/10.1080/15548627.2016.1166317>.
- [35] U. Nagaoka, K. Kim, N.R. Jana, H. Doi, M. Maruyama, K. Mitsui, F. Oyama, N. Nukina, Increased expression of p62 in expanded polyglutamine-expressing cells and its association with polyglutamine inclusions, *J. Neurochem.* 91 (2004) 57–68, <https://doi.org/10.1111/j.1471-4159.2004.02692.x>.
- [36] T. Ishii, T. Yanagawa, K. Yuki, T. Kawane, H. Yoshida, S. Bannai, Low micromolar levels of hydrogen peroxide and proteasome inhibitors induce the 60-kDa a170 stress protein in murine peritoneal macrophages, *Biochem. Biophys. Res. Commun.* 232 (1997) 33–37, <https://doi.org/10.1006/bbrc.1997.6221>.
- [37] T. Ishii, K. Itoh, S. Takahashi, H. Sato, T. Yanagawa, Y. Katoh, S. Bannai, M. Yamamoto, Transcription factor nrf2 coordinately regulates a group of oxidative stress-inducible genes in macrophages, *J. Biol. Chem.* 275 (2000) 16023–16029, <https://doi.org/10.1074/jbc.275.21.16023>.
- [38] S. Kageyama, S.R. Gudmundsson, Y.S. Sou, Y. Ichimura, N. Tamura, S. Kazuno, T. Ueno, Y. Miura, D. Noshiro, M. Abe, T. Mizushima, N. Miura, S. Okuda, H. Motohashi, J.A. Lee, K. Sakimura, T. Ohe, N.N. Noda, S. Waguri, E.L. Eskelinen, M. Komatsu, P62/sqstm1-droplet serves as a platform for autophagosome formation and anti-oxidative stress response, *Nat. Commun.* 12 (2021) 16, <https://doi.org/10.1038/s41467-020-20185-1>.